Mesoscopic metallosupramolecular texturing through hierarchic assembly

Sylvain Clair[1†], Stéphane Pons[1#], Harald Brune[1], Klaus Kern[1,2] and Johannes V. Barth[1,3]

[1] Institut de Physique des Nanostructures, Ecole Polytechnique Fédérale de Lausanne, CH-1015 Lausanne, Switzerland

[2] Max-Planck-Institut für Festkörperforschung, Heisenbergstrasse 1, D-70569 Stuttgart, Germany

[3] Departments of Chemistry and Physics & Astronomy, The University of British Columbia, Vancouver, B.C. V6T 1Z4, Canada

There is a strong current interest in improving fabrication and mesoscopic integration of functional nanosystems at surfaces. In particular new pathways need to be developed to provide methodologies for the synthesis and embedding of nanostructures across multiple length scales[1-4]. Here we introduce the combination of nanopatterning and controled metal-organic assembly to process prestructured metallic templates and generate arrangements at a higher hierarchical level. We present scanning tunneling microscopy results on the metal-directed assembly and mesoscopic organization of supramolecular architectures using a textured metal substrate, i.e., the Au(111) surface decorated with Fe or Co nanodot arrays. By tuning the local reaction conditions with codeposited dicarboxylate linker molecules distinct low-dimensional metallosupramolecular systems were synthesized, notably including regularly spaced Fe-terephthalate ribbons forming a grating whose extension is only limited by the substrate terrace morphology. These findings indicate that hierarchic assembly protocols blending physical nanopatterning[5-9] and supramolecular engineering[10-13] on surfaces are generally useful to fabricate nanomaterials with mesoscopic feature control.

The metal-directed self-assembly of functional molecules provides an extremely versatile strategy towards highly organized supramolecular systems[14-17]. Recent findings revealed that similar processes can be conducted at surfaces, where notably a series of metal-carboxylate architectures could be

generated, including mononuclear arrays, ladder structures and nanoporous 2D metal-organic coordination networks[13, 18-21]. However, up to now these systems have been obtained on homogenous substrates where typically organic layers were exposed to a flux of metal atoms. In order to control the spatial distribution of surface coordination architectures it is promising to explore prestructured surfaces, which - due to their intrinsic anisotropy, local concentration of reactants and site reactivity - allow to direct and confine the assembly, which is not possible with homogenous substrates. In this Letter we present a temperature-controlled scanning tunneling microscopy (STM) investigation on the steering of metallosupramolecular reticulation by using nanopatterned templates. This approach represents a demonstrator for a two-stage assembly strategy combining self-organized metal-on-metal growth followed by chemical processing. It is suggested that this methodology in general bears promise to fabricate low-dimensional functional nanosystems, to steer the formation of (metallo-)supramolecular assemblies, to study and control metal-molecule interfacing, or to structure template layers in the 100 nm regime for the handling of nanoscale objects.

Specifically, we employed regular lattices of transition metal dots by depositing small amounts of cobalt or iron on Au(111) at room temperature (RT). Due to preferred nucleation of metal islands at the elbow sites of the reconstructed surface[22] Fe or Co nanoarrays are readily obtained[23, 24]. Islands of monoatomic height evolve for Fe deposition, whereas bilayer dots are encountered with Co. In agreement with earlier findings, the STM data confirm that the Au(111) reconstruction is maintained, as shown with the exemplaric results reproduced in Figure 1. The superstructure is equivalent for the two elements. The lattice unit cell is nearly rectangular and ≈ 15 nm × 7 nm in size, however on smaller terraces and in the vicinity of defects substantial variations can occur. The typically employed amount of 0.1 ML Co or Fe produces islands comprising an average of ≈ 140 atoms. As we will show these islands represent nanoreservoirs for the metal-directed assembly of codeposited terephthalic acid molecules (1,4-benzoic acid – TPA). While the TPA molecules are entirely preserved on the bare Au(111) substrate where they form H-bonded sheets[25], they readily react with the available Co or Fe at room temperature (RT) or slightly elevated temperatures to form metal-organic nanostructures. The

respective complexation is a reaction between the carboxyl groups of the molecules and one or more transition metal adatoms (M), which eventually can be extracted from the islands. This implies deprotonation of the carboxyl group, i.e., an M-carboxylate evolves, and leads to formation of reticulated planar metal-organic arrangements. The resulting hydrogen atoms are expected to recombine into molecular hydrogen which is known to thermally desorb from noble metal substrates at the employed conditions[26]. The complexation reaction is therefore irreversible and can be represented formally by the following net equation: $2\ R{-}(COOH) + M \rightarrow (R{-}COO)_2{\cdots}M + H_2(\uparrow)$. Since the diffusivity of the complexes is limited and the metal-organic bond has appreciable strength, the connection between building blocks can be kept localized in the vicinity of the originally deposited metal dots. In contrast, the high mobility of TPA on bare Au(111) provides the necessary easy transport of the incoming molecule flux to the rims of the reactive metal islands.

The careful tuning of the molecular deposition conditions has been used to steer the formation of various metal-carboxylate arrangements. In particular we could obtain architectures comprising regularly spaced nanoporous islands, extended metallosupramolecular ribbons or one-dimensional systems. In general we observed a trend that Co gives rise to better ordered structures at the molecular scale than Fe, while the latter allows an easier steering at the mesoscopic level. The set of parameters that we optimized in order to obtain well-ordered architectures are the dosage (experiments were performed in the sub-monolayer range), the relative stoichiometry M : TPA, the thermal energy of the adspecies tuned by the temperature of the substrate during deposition and post-deposition annealing. With adequate temperature control it is notably possible to obtain surface nanostructures comprising (a) exclusively M-TPA compounds (M : TPA < 1) or (b) coexisting residual metal nanodots and reticulated M-TPA compounds (M : TPA > 1).

Figure 2a shows an STM image of the situation evolving upon exposing an Fe nanoarray on Au(111) to TPA with a stoichiometry of about 1 Fe atom per molecule, whereby the sample was maintained at T = 355 K during the molecular deposition. This procedure results in a complete dissolution of the Fe dots and the formation of irregular islands coexisting with the unperturbed chevron pattern of the Au(111)

substrate. While the presence of the latter clearly indicates that surface alloying between Fe and the substrate does not occur in the terraces, the irregular islands are clearly distinct from the extended close-packed quasi-hexagonal domains of H-bonded molecules characteristic for the adsorption of pure TPA[25]. The islands comprise open network features which are reminiscent of the ordering found in nanoporous Fe-carboxylate layers with TPA and related ditopic linear linkers on the square Cu(100) substrate[13, 18, 28]. It is thus concluded that they consist of Fe-diterephthalate arrangements stabilized by metal-organic reticulation. The size of the included characteristic open nanogrids is about 1×1.2 nm^2. Their relation to the metal-organic networks Cu(100) suggests that in a similar way the network nodes consist of di-iron centers surrounded by four molecules[13, 18, 28]. This is illustrated in the tentative model for an ideal Fe-TPA nanogrid with 1:1 M-molecule stoichiometry depicted in the inset in Fig. 2a. However, in contrast to the square Cu(100) substrate, the metal centers are not directly resolved by STM and the quasi-hexagonal lattice of Au(111) offers no match with an overlayer structure composed of rectangular motifs. As a consequence the Fe-TPA islands do not exceed 10 to 15 nm in size and present frequent distortions and misorientations. Indeed, we found that it is impossible to create extended regular nanogrid domains despite the smoothness of the substrate, indicating that while the strength of the metal-ligand interactions is appreciable, it is not sufficient to dictate the entire overlayer structure. In contrast with Co/Au(111) nanotemplates**,** the Fe-TPA system is more sensitive to the parameters stoichiometry and temperature and harder to control. While Co-TPA complexes organize in locally regular porous islands for the deposition parameters described above, Fe-TPA complex islands are rather disordered and give rise to a mixture between regular metal-organic grids and complicated irregular phases. Finally, the decoration of Au step edges is associated with local intermixing or coupling between Au and Fe, in agreement with findings for the pure Fe/Au(111) system[29]. This implies that Fe atoms can transport under the reaction conditions either directly via evaporation from the Fe dots or indirectly by release in the form of TPA-Fe complexes. In agreement - a general observation for Fe-TPA assemblies (see for example image 2a) with 1:1 stoichiometry - step decoration occurs preferentially at the bottom edges.

By lowering the annealing or deposition temperature and reducing the TPA concentration we succeeded in confining the complexation reaction. This is demonstrated by the STM image depicted in Figure 2b, which shows the result of a TPA dosage too small to form networks with all the iron available on the surface. As a consequence there is merely a partial dissolution of Fe islands and the cores of the metal islands remain at the Au(111) elbow sites. These residual Fe dots act as anchoring sites for reticulated metal-organic assemblies. All Fe islands are decorated by nanoporous irregular islands and chainlike features where the endgroups of the rodlike molecules are connected. The formation of these open structures again directly contrasts the compact packing in H-bonded pure TPA layers[25]. Consequently these arrangements must be stabilized by the incorporation of metal centers and reflect the limited surface mass transport of the reactants under the employed conditions. Thus the Fe-TPA nanogrid structure is poorly developed but the metal-organic islands coalesce and local bridges have evolved between them.

The connection between the localized complex islands is favored along the symmetry axis of the chevron pattern along the elbows. Two aspects can explain this growth anisotropy. Firstly, along this direction there is the shortest distance between two metallic dots and, indeed, we observed that the closer two metal-organic islands are the more likely they coalesce. In addition the substrate reconstruction pattern with its substantial lattice distortions at the elbows may induce directional molecular transport and orientations. By carefully controlling the molecular surface concentration thus regular metallosupramolecular ribbons with regular residual Fe anchoring sites can be fabricated. This is illustrated by the STM image in Figure 3 showing the mesoscopic ordering of a Fe-TPA ribbons induced by the chevron structure. The widths of the stripes in this architecture is usually around 5 to 10 nm while their lengths can reach hundreds of nanometers, i.e., they span entire terraces until they terminate at Au step edges. The aspect ratio of the ribbons therefore frequently exceeds 40 and by using vicinal transition metal decorated Au(111) substrates with the parallel step edges[7] macroscopically elongated metal-organic ribbons are to be expected.

By further fine tuning the deposition parameters we succeeded in the metal-directed assembly of monomolecular chains in the system Co-TPA on Au(111) as shown in Figure 4. Such metal-organic wires could be achieved at reduced molecular coverages with a limited success rate, and the 1D organizations coexist with nanogrid patches (not shown). They establish a connection between two adjacent dots and therefore do not exceed 10 nm in length. The exact internal structure and stoichiometry of these chains composed of M-terephthalate segments could not be determined. However, the distance between the molecular building blocks in the chain is by ≈ 10% increased with respect to that in H-bonded assemblies, which corroborates that it results from a complexation of TPA and Co where a distance of 0.2 nm between metal center and carboxylate oxygen atoms is expected. Moreover the 1D Co-TPA chains anchored by the Co dots are stable at RT, which reflects the appreciable strength of metal-ligand interactions, exceeding that of 1D TPA polymerization via hydrogen bonding. Accordingly monomolecular H-bonded chains can neither be obtained by molecular self-assembly at RT[25] nor are they encountered at cryogenic conditions.

In conclusion we have demonstrated that substrates patterned with transition metal nanoarrays can be successfully processed by tuning and spatially confining their reaction with functional molecular species. Methodologies employing such hierarchic assembly protocols are conceivable for a great variety of systems and can be applied at substrates with different symmetries, physical and chemical properties. They thus represent a promising route for the metallosupramolecular engineering of patterned templates by using linker molecules with specific functionalities. We expect that these findings contribute to an improved control of matter at the nanoscale, the mesoscopic organization of template structures, and the design of supramolecular functional systems.

Experimental Section

The experiments were performed with a ultrahigh vacuum system (base pressure $< 3 \times 10^{-10}$ mbar) comprising a home-built STM working at variable temperature (400 – 5 K) as described in ref. [27]. The data presented were recorded in the constant current mode; indicated voltages refer to the sample bias. The Au(111) substrate was prepared by repeated cycles of RT Ar bombardment (≈ 5 μA/cm^2 at 800 eV) followed by annealing at 900 K. Terraces larger than 100 nm were commonly observed. Iron and cobalt

were evaporated at low deposition rates (< 1/3 ML per minute). One ML of metal refers to a hypothetical perfect commensurate monatomic layer on the gold surface. TPA molecules (FLUKA, purity > 99 %) were evaporated using a Organic Molecular Beam Deposition (OMBD) source, by heating a crucible to 150 °C - the pertaining evaporation rate was ≈ 1 ML (complete monomolecular layer) per minute[27]. A metal–to–TPA stoichiometry of 1:1 corresponds to a coverage ration of ≈ 9 : 1.

Acknowledgements

Work supported by the Swiss National Science Foundation (as part of the European Science Foundation EUROCORES Programme SONSs) and the EC Sixth Framework Programme (as part of the STREP BioMACH). Images were partly processed with the public domain program WSxM, available at http://www.nanotec.es.

† present address : RIKEN, The Institute for Physical and Chemical Research, 2-1 Hirosawa, Wako, Saitama 351-0198, Japan. E-mail: sclair@riken.jp.

present address : Laboratoire de Physique des Matériaux, Université Henri Poincaré, Nancy, F-54506 Vandoeuvre-lès-Nancy, France. E-mail: stephane.pons@lpm.u-nancy.fr.

Figures

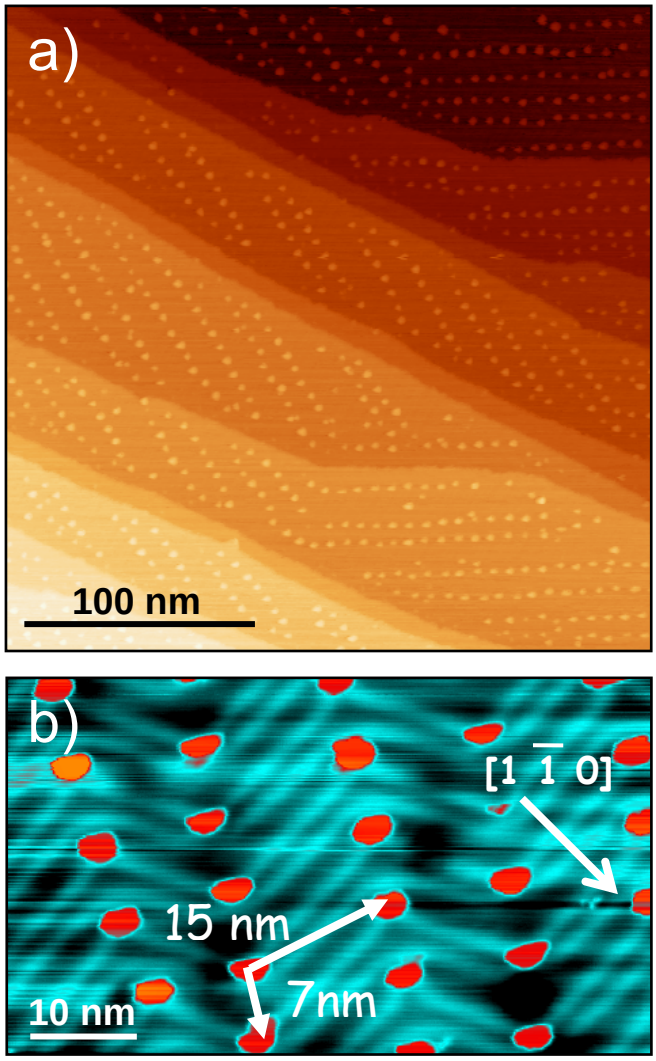

Figure 1 STM images of Au(111) template with the chevron reconstruction dislocation pattern decorated with transition metal arrays reflecting preferential nucleation at elbow sites. a) Bilayer cobalt islands forming regular lattices on several terraces (0.14 ML Co deposited at RT; image size 280 × 280 nm^2, V = - 25 mV, I = 0.8 nA, recorded at RT). b) Monolayer high Fe dots (red spots) in a single terrace with the characteristic double lines of the reconstruction simultaneously resolved. The unit cell of the regular lattice is ≈ 15 nm × 7 nm in size. (0.1 ML Fe deposited at RT; image size 60 × 35 nm^2, V = 20 mV, I = 1 nA, recorded at 5 K).

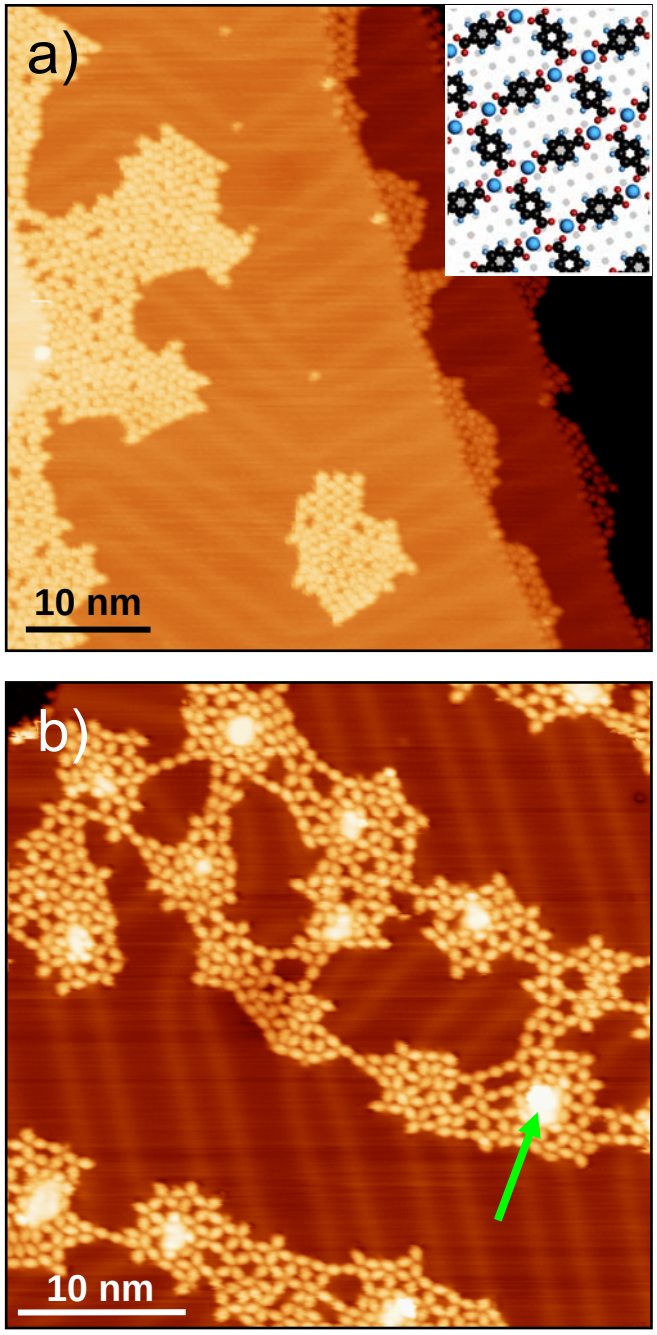

Figure 2 Controling the Fe – TPA complexation reaction. a) Complete dissolution of Fe islands for a Fe – TPA stoichiometry of ≈ 1:1 following deposition of TPA on the Fe nanoarrays at 355 K. Fe-carboxylate islands preferentially decorate step edges (image size 51 x 51 nm^2, V = -2.5 V, I = 0.5 nA, recorded at 5 K). The inset shows a tentative model for an ideal Fe-TPA nanogrid where at each di-iron center the endgroups of four molecular linkers come together. b) Localized reaction with TPA deposition at 325 K and 10 minute post-deposition annealing at 330 K. The Fe islands are only partially comsumed in the complexation reaction, however the resulting nanogrid structure reflects selective growth of metal-organic islands at residual Fe dots (cf. Fe island indicated by arrow; 0.1 ML Fe, 0.25 ML TPA; image size 38 × 38 nm^2, V = 1.5 V, I = 0.2 nA, recorded at 5 K).

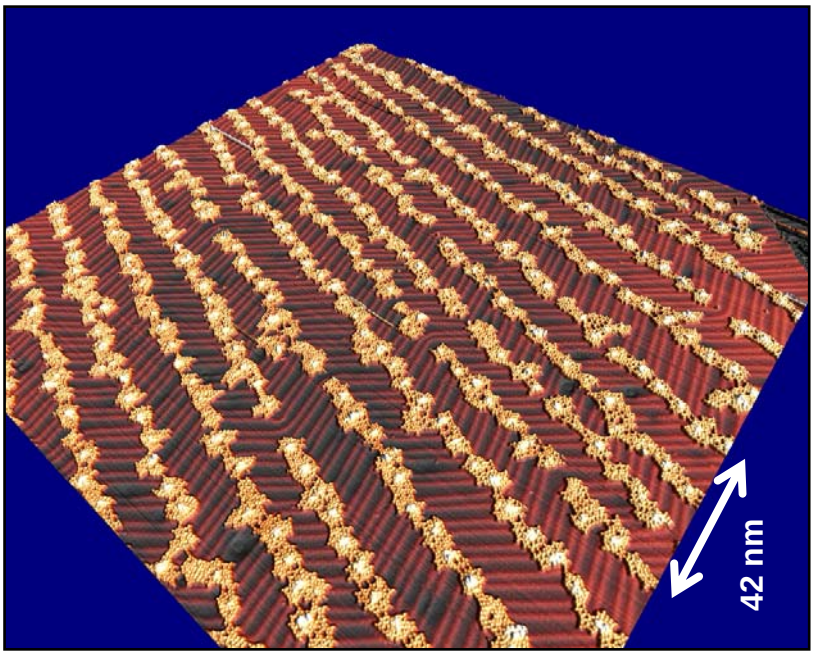

Figure 3 Mesoscopic ordering of metallosupramolecular ribbons. Fe-terephthalate linkages evolve between next-neighbor Fe-islands following TPA exposure. The residual Fe dots at the elbow sites of the reconstruction anchor the pattern, i.e., the spatial distribution of the Fe dots steers the organization. The length of the metal-organic ribbons is in the several hundred nm range, with typical widths of 5 - 10 nm. The respective aspect ratio of the stripes is commonly better than 20 to 40 (image size 220 × 220 nm^2, V = - 1.5 V, I = 0.8 nA, recorded at 5 K; 0.1 ML Fe exposed to 0.25 ML TPA at 325 K, i.e., fourfold Fe excess with respect to ideal 1:1 nanogrid stoichiometry).

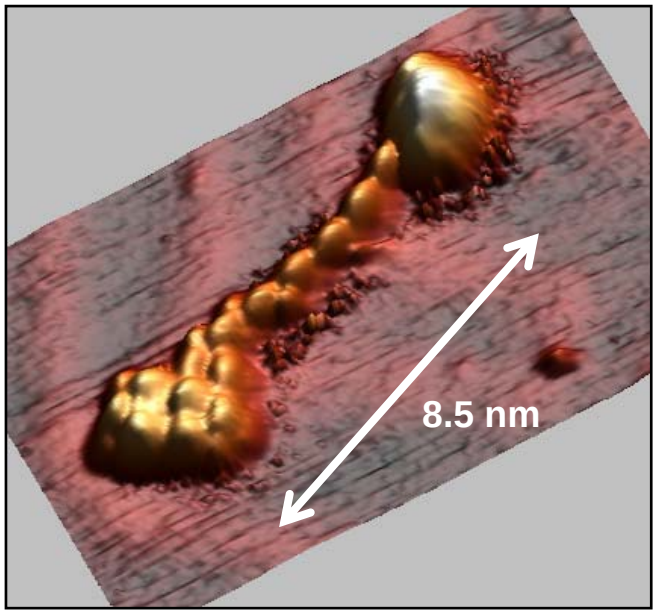

Figure 4 Monomolecular Co-TPA 'wire' linking two cobalt nanodots. The Co island rims are also decorated by molecules. This 1D structure coexists on the surface with regions covered by nanogrids (doses: 0.2 ML Co, 0.2 ML TPA; sample kept at 360 K during TPA deposition; image size 15 × 8 nm^2, V = - 700 mV, I = 0.6 nA, recorded at RT).

References

[1] T. Ogino, H. Hibino, T. Homma, Y. Kobayashi, K. Prabhakaran, K. Sumitomo, H. Omi, *Acc. Chem. Res.* **1999**, 447.
[2] Y. N. Xia, J. A. Rogers, K. E. Paul, G. M. Whitesides, *Chem. Rev.* **1999**, *99*, 1823.
[3] H. Cölfen, S. Mann, *Angew. Chem. Int. Ed.* **2003**, *42*, 2350
[4] C. Lin, C. R. Kagan, *J. Am. Chem. Soc.* **2003**, *125*, 336
[5] K. Kern, H. Niehus, A. Schatz, P. Zeppenfeld, J. George, G. Comsa, *Phys. Rev. Lett.* **1991**, *67*, 855.
[6] H. Brune, M. Giovannini, K. Bromann, K. Kern, *Nature* **1998**, *394*, 451.
[7] V. Repain, G. Baudot, H. Ellmer, S. Rousset, *Europhys. Lett.* **2002**, *58*, 730
[8] M. Corso, W. Auwärter, M. Muntwiler, A. Tamai, T. Greber, J. Osterwalder, *Science* **2004**, *303*, 217
[9] R. Otero, Y. Naitoh, F. Rosei, P. Jiang, P. Thostrup, A. Gourdon, E. Laegsgaard, I. Stensgaard, C. Joachim, F. Besenbacher, *Angew. Chem. Int. Ed.* **2004**, *43*, 2092
[10] J. V. Barth, J. Weckesser, C. Cai, P. Günter, L. Bürgi, O. Jeandupeux, K. Kern, *Angew. Chem. Int. Ed.* **2000**, *39*, 1230.
[11] J. A. Theobald, N. S. Oxtoby, M. A. Phillips, N. R. Champness, P. H. Beton, *Nature* **2003**, *424*, 1029
[12] T. Yokoyama, S. Yokoyama, T. Kamikado, Y. Okuno, S. Mashiko, *Nature* **2001**, *413*, 619
[13] S. Stepanow, M. Lingenfelder, A. Dmitriev, H. Spillmann, E. Delvigne, N. Lin, X. Deng, C. Cai, J. V. Barth, K. Kern, *Nature Mat.* **2004**, *3*, 229.
[14] D. Philp, J. F. Stoddart, *Angew. Chem. Int. Ed.* **1996**, *35*, 1154
[15] S. Leininger, B. Olenyuk, P. J. Stang, *Chem. Rev.* **2000**, *100*, 853.
[16] J. M. Lehn, *Proc. Nat. Acad. Sci.* **2002**, *99*, 4763.
[17] B. J. Holliday, C. A. Mirkin, *Angew. Chem. Int. Ed.* **2002**, *40*, 2022.
[18] A. Dmitriev, H. Spillmann, N. Lin, J. V. Barth, K. Kern, *Angew. Chem. Int. Ed.* **2003**, *41*, 2670
[19] J. V. Barth, J. Weckesser, N. Lin, S. Dmitriev, K. Kern, *Appl. Phys. A* **2003**, *76*, 645.
[20] H. Spillmann, A. Dmitriev, N. Lin, P. Messina, J. V. Barth, K. Kern, *J. Am. Chem. Soc.* **2003**, *125*, 10725
[21] A. Dmitriev, H. Spillmann, M. Lingenfelder, N. Lin, J. V. Barth, K. Kern, *Langmuir* **2004**, *41*, 4799.
[22] J. V. Barth, H. Brune, G. Ertl, R. J. Behm, *Phys. Rev. B* **1990**, *42*, 9307.
[23] B. Voigtländer, G. Meyer, N. M. Amer, *Phys. Rev. B* **1991**, *44*, 10354.
[24] J. A. Stroscio, D. T. Pierce, R. A. Dragoset, P. N. First, *J. Vac. Sci. Tech.* **1992**, *10*.
[25] S. Clair, S. Pons, A. P. Seitsonen, H. Brune, K. Kern, J. V. Barth, *J. Phys. Chem. B* **2004**, *108*, 14585
[26] X.-L. Zhou, J. M. White, B. E. Koel, *Surf. Sci.* **1989**, *218*, 201
[27] S. Clair, PhD thesis, EPF (Lausanne), **2004**.
[28] M. A. Lingenfelder, H. Spillmann, A. Dmitriev, S. Stepanov, N. Lin, J. V. Barth, K. Kern, *Chem. Eur. J.* **2004**, *10*, 1913.
[29] S. Shiraki, H. Fujisawa, M. Nantoh, M. Kawai, *J. El. Spectr. Rel. Phen.* **2004**, *137-140*, 177.

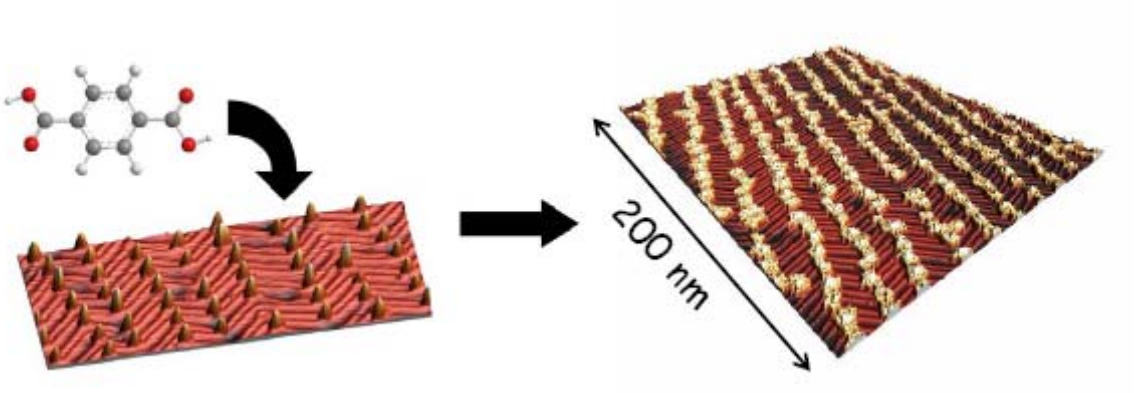

TOC

In a two-stage assembly protocol regularly spaced transition metal islands on the Au(111) surface are employed to steer the formation and organization of metallosupramolecular nanosystems.

Keywords:
coordination compounds · nanomaterials · nanochemistry · scanning tunneling microscopy · self-assembly